

A Simplified Electric Vehicle Battery Degradation Model Validated with the Nissan LEAF e-plus 62-kWh

Marinelli, Mattia; Calearo, Lisa; Engelhardt, Jan

Published in: Proceedings of 6th International Electric Vehicle Technology Conference

Publication date: 2023

Document Version Publisher's PDF, also known as Version of record

Link back to DTU Orbit

Citation (APA): Marinelli, M., Calearo, L., & Engelhardt, J. (2023). A Simplified Electric Vehicle Battery Degradation Model Validated with the Nissan LEAF e-plus 62-kWh. In *Proceedings of 6th International Electric Vehicle Technology Conference*

General rights

Copyright and moral rights for the publications made accessible in the public portal are retained by the authors and/or other copyright owners and it is a condition of accessing publications that users recognise and abide by the legal requirements associated with these rights.

• Users may download and print one copy of any publication from the public portal for the purpose of private study or research.

- You may not further distribute the material or use it for any profit-making activity or commercial gain
- You may freely distribute the URL identifying the publication in the public portal

If you believe that this document breaches copyright please contact us providing details, and we will remove access to the work immediately and investigate your claim.

A Simplified Electric Vehicle Battery Degradation Model Validated with the Nissan LEAF e-plus 62-kWh

Mattia Marinelli ¹⁾, Lisa Calearo ²⁾, Jan Engelhardt ¹⁾

 Technical University of Denmark (DTU), Department of Wind and Energy Systems, Risø campus, Roskilde, Denmark E-mail: <u>matm@dtu.dk</u>; <u>janen@dtu.dk</u>
 Ramboll Danmark A/S, Copenhagen, Denmark E-mail: <u>licl@ramboll.com</u>

ABSTRACT: Validated degradation models are needed to ensure optimized operation of battery systems. This paper presents a simplified electric vehicle battery degradation model, which estimates the degradation based on vehicle usage daily values. The model quantifies calendar and cycle degradation based on battery temperature, State-of-Charge and odometer. The model results are compared against two datasets of 2.5 years obtained with a LEAF e-plus: on-board State-of-Health readings retrieved from the battery management system and capacity estimations assessed while monitoring battery full recharges. The results show that, after 2.5 years, the model is well-aligned with the capacity estimations, while the on-board readings estimate the State-of-Health 1.3% lower. The obtained State-of-Health from the model after 2.5 years is equal to 95.6%, with calendar degradation being the major driver for the degradation cumulated so far.

KEY WORDS: Battery pack; Calendar ageing; Cycle Ageing; Degradation models; Electric vehicles; State-of-Health; Testing.

Variables						
t	Time (s)					
SoC	State-of-Charge (%)					
SoH _{read}	State-of-Health by the on-board readings (%)					
SoH _{model}	State-of-Health by the model (%)					
SoH _{est}	State-of-Health by the capacity estimation (%)					
Odo	Odometer (km)					
$T_{\rm b}$	Battery temperature (°C)					
Vb	Battery voltage (V)					
Ib	Battery current (A)					
Pb	Battery power (W)					
Eb	Battery energy (Wh)					
V _{ch}	DC charger voltage (V)					
Ich	DC charger current (I)					
$E_{\rm ch}$	DC charger energy (Wh)					
V _{aux}	Electric vehicle auxiliary voltage (V)					
I _{aux}	Electric vehicle auxiliary current (I)					
E_{aux}	Electric vehicle auxiliary energy (Wh)					
E _{net}	Net energy charged in a lab session (Wh)					
$q_{ m cal}$	Cumulated calendar degradation (%)					
$q_{ m cycl}$	Cumulated cycle degradation (%)					
Q	Battery Ah capacity (Ah)					
f	Pre-exponential factor for calendar degradation					
η	Driving specific energy consumption (Wh/km)					
$\Delta t_{driving}$	Driving time in a specific period (s)					

LIS OF VARIABLES AND PARAMETERS

Parameters						
$Q_{ m nom}$	Battery nominal Ah capacity equal to 176.4 Ah					
$V_{\rm nom}$	Battery nominal voltage equal to 350.4 V					
$E_{\rm nom}$	Battery nominal energy equal to 61.8 kWh					
E_{a}	Activation energy equal to 24.5 kJ/mol					
R	Gas constant equal to 8.314 J/(mol·K)					
а	Empirical coeff. equal to 8.6*10 ⁻⁶ 1/(Ah·K ²)					
b	Empirical coeff. equal to 5.1*10 ⁻³ 1/(Ah·K)					
С	Empirical coeff. equal to 0.76 1/(Ah)					
d	Empirical coeff. equal to $6.7*10^{-3} 1/(K \cdot s)$					
е	Empirical coeff. equal to 2.34 s					

1. INTRODUCTION

1.1 Background

Electric vehicle (EV) is becoming a dominant technology in the transportation sector. Its optimal usage and integration in the electric grid have been widely assessed in a large variety of studies [1]. Battery degradation, however, remains a major concern for electric vehicle users: proper understanding and quantification of its main drivers can enable optimized operation and charging process [2]. Moreover, it can also facilitate the usage of the battery for services not strictly related to driving, such as vehicle-to-grid (V2G) [3], [4]. In power system applications, it is common to use simplified battery pack models to reduce simulation time and model complexity. This is also because cells within a battery pack

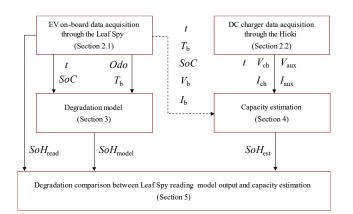
may not always experience identical conditions [5]. As a result, degradation at the pack level may not necessarily correspond directly to the degradation of individual cells [6]. Traditionally, battery degradation is divided into cycle and calendar, with the first one driven by temperature, discharge rate and cycles, while the latter being dominated by time, temperature and SoC [7]. Despite the literature providing different models of single battery cells, validated battery pack models are scarce.

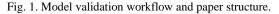
1.2 Objectives and contributions

The objective of the paper is to present a simplified EV battery degradation model that can capture the overall trend without requiring extensive datasets. The model is validated against:

- on-board State-of-Health readings retrieved from the battery management system, using the method presented in [8];
- capacity estimation obtained while monitoring battery full recharges, using the methodology presented in [9].

The overall workflow to validate the model is presented in Fig. 1, along with data and measurements utilized in each step. The figure also serves as a guide for the rest of the paper. Section 2.1 discusses the data acquired through the OBD-II reader and an application named Leaf Spy. Data acquired via a Hioki datalogger of the DC charger used to perform the capacity estimations is discussed in Section 2.2. The degradation model is presented in Section 3, while the capacity estimation method is summarized in Section 4. In Section 5, the comparison between State-of-Health output of the model, the one derived by the capacity estimations and the one retrieved by the Leaf Spy is reported.





2. DATA ACQUISITION

2.1. EV on-board data

The Leaf Spy application allows for the acquisition of secondbased measurements of a large set of quantities, retrieved through an OBD-II reader. Although all driving sessions have been recorded from the vehicle, to limit the dataset and make the method easier to apply only two instances from each day are used: one in the morning before the car is being driven and one in the evening before the car is being parked for the night. For the modelling part, the following quantities are mainly relevant: time, SoC, odometer, battery temperature. For the capacity measurement, the following two quantities are considered additionally: battery voltage and current.

As previously presented in [8], a series of key quantities is acquired from the battery management system (BMS), including SoH readings. Table 1 reports battery usage indicators like mean *SoC* and T_b along with the distance driven for the 90-day periods.

Periods SoH_{read} SoH_{read} Mean Mean T_{b} . Driven								
Terious	Sonread			-				
		reset	SoC	(°C)	distance (km)			
27/10/20	100.00%	-	49%	8.6	2631			
25/01/21	99.46%							
25/01/21	99.46%	-0.00%	60%	6.8	3036			
25/04/21	99.25%							
25/04/21	99.32%	+0.07%	58%	19.5	4647			
23/07/21	98.77%							
24/07/21	99.39%	+0.62%	66%	18.8	3968			
21/10/21	99.04%							
23/10/21	97.35%	-1.69%	61%	8.2	3356			
19/01/22	97.25%							
23/01/22	95.50%	-1.75%	62%	7.4	3227			
21/04/22	95.41%							
22/04/22	95.40%	-0.01%	63%	19.4	5079			
19/07/22	95.07%							
20/07/22	93.93%	-1.14%	58%	19.8	4796			
17/10/22	93.59%							
17/10/22	94.22%	+0.63%	61%	8.5	3077			
14/01/23	94.14%							
16/01/23	94.34%	+0.20%	55%	5.1	1605			
18/03/23	94.32%							
(ongoing)								

The 90-day window is chosen to highlight the recurring SoH_{read} resets performed by the vehicle BMS. Over the 2.5-year period of usage of the EV, the average battery temperature stands at 12.6 °C against an average ambient temperature of 9.0 °C. Charging processes avoid high SoC for long periods and are mostly based on slow charging. A time weighted average SoC equal to 61% is observed along with a total driven distance of 35538 km.

6th International Electric Vehicle Technology Conference 2023

The daily breakdown of the driven distance is reported in Fig. 2. The average distance per day is equal to 42 km and for 135 days out of the 838 days analyzed the car was not driven. For 821 days out of 838, the car drove less than 200 km/day, which means that fast charging sessions did mostly happen in the remaining 17 days, when the daily driven distance was more than 200 km.

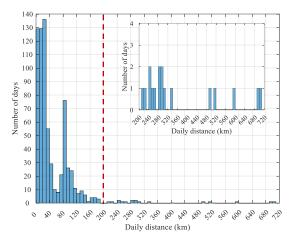


Fig. 2. Daily distance driven between 01/12/2020 (the day that the car was registered in Denmark) and 18/03/2023.

2.2. DC charger data

Every 3-4 months, the car is driven to the laboratory to perform capacity estimations: the EV is completely discharged until the minimum voltage allowed by the BMS is reached (see Fig. 3).



Fig. 3. The LEAF e-plus under test in the laboratory at DTU.

Afterwards, a monitored recharge takes place: the DC power used to charge the vehicle is measured at the charger terminal. The power needed to supply the auxiliary systems of the EV is separately measured and is subtracted from the total to assess solely the energy used to recharge the main battery. Second-based values from the DC charger and from the 12 V bus of the EV are measured with dedicated DC voltage and current clamps and acquired through a Hioki datalogger.

3. DEGRADATION MODEL

3.1. Model structure

The degradation model, realized in Matlab-Simulink, accounts separately calendar and cycle degradation and is derived from the formulation presented in [10].

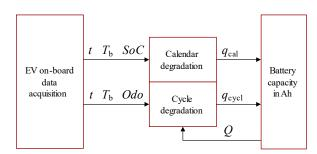


Fig. 4. Synthetic overview of the degradation model.

Calendar degradation is calculated by using battery temperature and SoC: two values per day are used and are linearly interpolated over time. Since only average values are considered, charge and discharge processes taking place throughout the day are not captured. This assumption is made to limit the simulation time of the model without compromising the validity of the results, considering that calendar degradation dynamics evolve over long time horizons.

Cycle degradation is, instead, based on the daily distance driven, in km, which is then used to assess the corresponding energy consumed, in kWh. The model further considers the temperature of the battery pack. The effect of repeated fast charging on both temperature and energy intensity is not fully captured. However, when active cooling is not present, as in the case of the LEAF, the battery temperature will remain high also few hours after the last fast charge [8]. Whereas during low-power charging sessions, the model will not lose accuracy since the temperature is marginally affected. Degradation values, q_{cal} and q_{cycl} , are used to compute the actual battery capacity, Q, in Ah, and the normalized quantity, SoH_{model} :

$$Q = Q_{nom} \cdot (100\% - q_{cal} - q_{cycl}) \tag{1}$$

$$SoH_{model} = 100\% - q_{cal} - q_{cvcl} \tag{2}$$

3.2. Calendar degradation

Calendar degradation is based on Arrhenius formulation, to consider temperature dependency. The resulting cumulated degradation, expressed in percentage, is computed as follows:

$$q_{cal} = \frac{1}{\Delta t} \int \left(f \cdot exp^{\frac{-E_a}{R \cdot T_b}} \cdot \sqrt{t} \right) - \left(f \cdot exp^{\frac{-E_a}{R \cdot T_b}} \cdot \sqrt{t - \Delta t} \right) dt,$$
(3)

where Δt is equal to 1 second, while *t* is measured in days. The battery temperature, *T*_b, is reported as absolute temperature. The pre-exponential factor, *f*, is based on the piecewise formulation reported in Table 2 and is derived from experimental estimations for NMC cells, presented in [11]. Several trends can be observed: a rising value for SoC until 30%, followed by a rather constant area until 60%, where the increase of the pre-exponential factor, and therefore calendar degradation, is limited. Between 60% and 70%, there is a steep increase, which is again followed by another rather constant area between 70% and 90%.

Table 2. Pre-exponential factor as a function of SoC

SoC	0%	10%	20%	30%	40%
f	1500	2000	2500	3000	3100
50%	60%	70%	80%	90%	100%
3100	3600	6100	6100	6500	7400

This means that keeping a low SoC helps the battery to preserve its capacity. The effects of SoC and battery temperature are graphically presented in Fig. 5 over a period of 10 years.

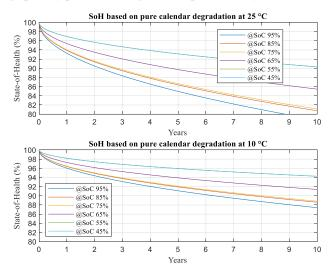


Fig. 5. SoH based on pure calendar degradation under various SoC and at two constant temperatures (25 $^{\circ}$ C and 10 $^{\circ}$ C).

Additional degradation caused by cycles is not considered in this case. Besides the influence of SoC levels, it is clear how high temperature negatively affects lifetime. If one looks at the purple curves in the two plots (*SoC* = 65%), it can be seen how the SoH at the 10-year mark goes from 91% at 10 °C down to 86% at 25 °C

and would get further down to 76% if the battery was constantly kept at 40 $^{\circ}$ C.

3.2. Cycle degradation

Cycle degradation is based on the following formulation, where cumulated degradation expressed in percentage is reported:

$$q_{\text{cycl}} = \int \left(a \cdot T_b^2 + b \cdot T_b + c \right) \cdot exp^{(d \cdot T_b + e) \cdot \frac{I_b}{Q}} \cdot \frac{I_b}{Q \cdot 3600} dt \quad (4)$$

With battery temperature, T_b , reported in absolute values; actual battery capacity, Q, reported in Ampere-hour and by considering only discharging currents for I_b . Coefficients reported in equation (2) are based on the measurements described in [12].

Since this paper intends to further simplify the formulation for cycle degradation by only using daily driving measurements, the battery current, I_b , used in (4) is derived from odometer readings. By knowing the driven distance during a specific day and the related driving specific energy consumption, it is possible to compute the energy used during the driving session. Knowing the driving time during the period and given the battery pack nominal voltage, V_{nom} , the current can be obtained as indicated in (4):

$$I_{\rm b} = \frac{Odo \cdot \eta}{\Delta t_{driving}} \cdot \frac{1}{V_{nom}}$$
(5)

The effects of driven distance and battery temperature are graphically presented in Fig. 6 over a period of 10 years. An average driving specific energy consumption, η , of 180 Wh/km is considered. Additional degradation caused by calendar is not accounted for in this case. It is clear how cycle degradation plays a minor role in the overall degradation. Under ideal temperature, which for cycle degradation is 25 °C, the cumulated wear predicted by the model is expected to be less than 1% after 10 years, even when considering a very intense driving usage of 50000 km/year, which roughly corresponds to 150 full cycles for the 61.8-kWh battery investigated.

Colder and higher temperatures negatively affect cycle degradation: with a battery temperature of 10 °C, cycle degradation gets five times larger. As discussed in [13], cycle degradation has a quadratic dependency on temperature with a minimum around 25 °C: degradation at 10 °C is as high as at 40 °C, therefore, the lower plot of Fig. 6 gives a good indication of what the cycle degradation could be with a temperature of 40 °C.

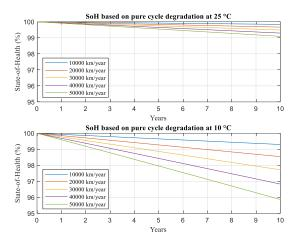


Fig. 6. SoH based on pure cycle degradation with various yearly driving and at two constant temperatures (25 °C and 10 °C).

It is worth noting how, on average, cars in Europe are driven between 9000 and 15000 km/year, depending on the country. This means that even under intense driving conditions, the battery could still be used for other purposes such as V2G applications, without considerable downside from a degradation perspective.

4. CAPACITY ESTIMATION

4.1. Capacity estimation method

As mentioned in Section 2.2, the EV is subject to regular fullcharging sessions to estimate the available charging capacity. During the charging session, the following quantities are calculated based on the measurements acquired by the datalogger: charged DC energy, and energy consumed in the auxiliary.

The energy provided by the DC charger, E_{ch} , is computed by integrating over time the measured V_{ch} and I_{ch} , provided by the Hioki datalogger. The energy consumed by the EV auxiliary, E_{aux} , is computed by integrating over time the respective voltage and current measured at the 12 V bus, acquired by the Leaf Spy. The net energy charged is therefore defined as the difference between E_{ch} and E_{aux} . The resulting value is finally normalized by the battery nominal capacity, E_{nom} , to obtain SoH_{est} .

Throughout the charging sessions, also the following quantities are recorded to ensure consistency and replicability; however, they are not used to modify the final *SoH*est: battery temperature, voltage and SoC. Specifically, battery temperature, although it cannot be actively controlled, is observed to ensure consistency among the different sessions. To warm up the battery in winter months, the measurements were planned during non-particularly cold days and the EV was driven for 2 hours on the highway. This was also needed to discharge the battery to approximately 10-15% SoC, before having the final discharge by using the onboard heating for the following 3-4 hours inside the laboratory. In this way the battery had enough time to reach at least 14 °C. By the end of the charging session, which normally lasts 8 hours, the battery reached 24 °C. Finally, to keep at a minimum the influence of charging losses inside the battery, a 23-A DC charger is used, which, compared to the battery nominal capacity of 176.4 Ah, implies a C-rate of 0.13. Details on the capacity measurement technique applied on different car types are available in [9].

4.2. Capacity estimation results

Table 3 summarizes the most relevant quantities acquired during the capacity estimation sessions. The battery voltage, V_b , at the beginning of the charging session could not always be kept at the same value, because in the last few percentage points of SoC, the cells, which are normally balanced in the range of 10-20 mV, tend to become unbalanced (see Fig. 7).

As discussed in [8], the battery pack consists of triplets of cells, each of 58.8 Ah, wired in a series of 96, for a total of 288 cells. As soon as the first triplet reaches 2.85 V, the BMS prevents further discharge. However, as indicated in Table 3, normally the voltage ends up between 286 and 302 V. The final voltage at the end of the session is more predictable as the cells will be charged until reaching a value between 4.18 V and 4.20 V, therefore the overall battery voltage will be between 402 V and 403 V. The corresponding minimum SoC ranges between 0% and 2%, while the maximum between 96% and 98%. Finally, the fact that not the whole 100% SoC is made available for the charging session is not considered for the sake of determining *SoH*est.

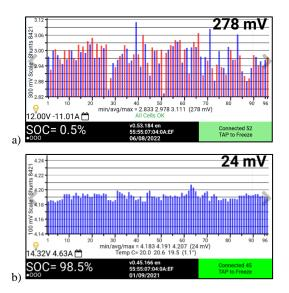


Fig. 7. The 96 cell triplet voltages displayed at the end of a discharging session (a) and at the end of a charging session (b).

Date	18/12/20	23/07/21	20/08/21	17/09/21	22/10/21	22/02/22	31/03/22	06/08/22	27/10/22	02/02/23
SoC start	1.74%	1.57%	2.41%	1.76%	0.50%	0.00%	0.00%	0.51%	1.13%	0.60%
SoC end	96.54%	96.20%	96.55%	96.87%	96.22%	96.21%	96.15%	98.12%	97.93%	96.94%
$V_{\rm b}$ start (V)	302.7	299.2	287.7	288.5	291.7	291.4	290.4	286.4	288.4	288.5
$V_{\rm b}$ end (V)	402.7	402.5	403.0	402.8	402.9	402.9	402.9	403.2	403.2	403.2
$T_{\rm b}$ start (°C)	19.0	29.1	24.9	26.4	18.0	17.5	15.3	25.3	19.2	14.3
$T_{\rm b}$ end (°C)	26.6	32.7	29.9	31.1	25.6	24.8	24.1	30.7	26.3	22.8
Charge duration	08:07	08:00	07:54	07:52	07:50	08:02	08:02	08:00	07:44	07:54
$E_{\rm ch}$ (Wh)	62224	60944	61401	60792	60662	60531	60993	60432	60387	60338
$E_{\rm aux}$ (Wh)	1084	985	1000	1069	1032	1042	1113	1054	1021	1000
$E_{\rm net}$ (Wh)	61140	59959	60401	59723	59630	59489	59880	59378	59366	59338
SoH _{est}	98.92%	97.01%	97.72%	96.62%	96.47%	96.24%	96.88%	96.07%	96.05%	96.00%

Table 3. Summary results of the capacity estimations.

A graphical overview of the battery key quantities like, current, voltage, power and SoC measured during the charging session taking place on 02/02/2023 are reported in Fig. 8 and Fig. 9.

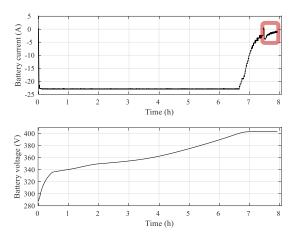


Fig. 8. Measured battery current and voltage.

The charging current is kept at 23 A until the SoC reaches 92%, at that point the topping phase begins, and the voltage slowly increases from 400 V to 402 V, while the current decreases until it reaches 2 A, with a SoC around 96%. Here, the final tail of the charging curve is performed by using the on-board AC charger. Less than 400 Wh are charged in the last phase (highlighted in red in the first plot of Fig. 8). The charging power starts at 6.7 kW at the very beginning, and it peaks at 9.2 kW before the charging session changes from constant current to constant voltage mode. The SoC increases linearly as long as the current is constant, while the increase gets progressively slower during the constant voltage mode. Further details on the charging modes of the LEAF are provided in [14].

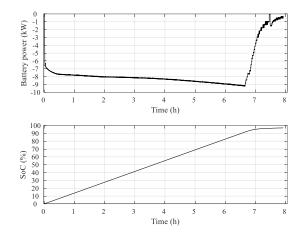


Fig. 9. Measured battery power and SoC.

Finally, Fig. 10 displays air and battery temperature from three different sensors inside the pack. When the EV entered the lab at 9:20, the battery temperature was at 7 °C and it slowly increased until 14 °C during the following 3 hours, when completing the discharging phase. The ambient temperature in the laboratory was kept constant at 21 °C. Interestingly, when the charging session started at 12:20, the battery temperature dips slightly in the first hour, before Joule losses take over and, together with the contribution from surrounding environment, contribute to the heating of the battery pack.

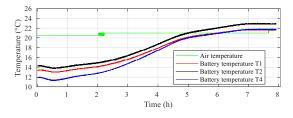


Fig. 10. Measured air and battery temperatures.

6th International Electric Vehicle Technology Conference 2023

5. DEGRADATION COMPARISON

The degradation estimated by the model is here discussed and compared with the one obtained by capacity estimations and onboard readings. The upper plots in Fig. 11 report the daily values acquired through the OBD-II for battery temperature, SoC and odometer, which are used to feed the degradation model. The lower plot shows the comparison between the model output in red, the on-board readings in blue and the measured capacity in green circles. The capacity values have an uncertainty of $\pm 1\%$ due to the measurement equipment.

The results show that, after 2.5 years, the model is well-aligned with the capacity estimations, while the on-board readings estimate the State-of-Health 1.3% lower. However, it is unclear to the authors how reliable the measurements from the OBD-II reader are, since they are provided by a third-party application. Another possible source of deviation can be caused by the estimation algorithm itself, which could be more conservative by overestimating the degradation.

It is worth reminding that, although the LEAF e-plus nominal capacity is 61.8 kWh, the car has a declared net capacity of 56 kWh. This implies that if 100% SoH is assigned to 61.8 kWh, once SoH reaches 90.6%, the battery capacity will be equal to 56 kWh. One could argue whether 56 kWh should be taken as the starting point and therefore be assigned a SoH equal to 100%. If this is the case, however, it would create a problem in using the capacity estimation as a comparison, since it would lead to a SoH larger than 100%: the last capacity value obtained at the end of the investigated period is 96.0%, which is equal to 59.3 kWh.

Finally, it is interesting to highlight how the on-board degradation algorithm has recurring major updates every 90 days, as already pointed out in [8].

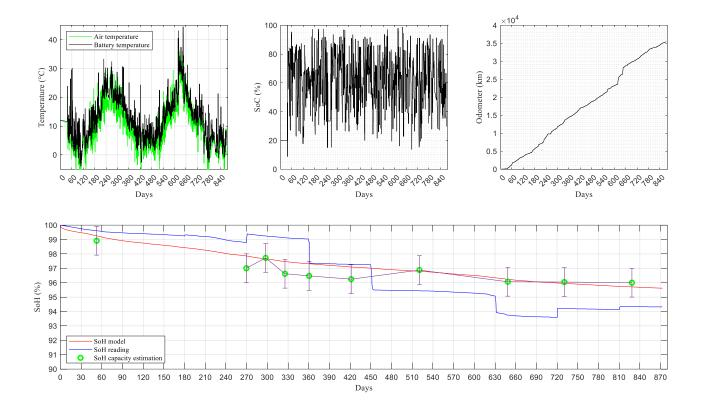


Fig. 11. Historical values used to feed the degradation model: T_b (top left), *SoC* (top center), *Odo* (top right). Air temperature is reported in the first plot just for comparison with the battery temperature, though it is not used in the model. State-of-Health comparison between model, on-board readings, and capacity estimations (lower plot).

6. CONCLUSION AND FUTURE WORK

The paper discussed and validated a simplified EV battery degradation model based on sparsely populated datasets. The model relies on two daily measurements of battery temperature, SoC and odometer. The model has been described in analytical terms and compared against two datasets of 2.5 years: on-board SoH readings retrieved from the battery management system, and capacity estimation obtained while monitoring battery full charges.

The results show that, after 2.5 years, the model is well-aligned with the capacity estimations, while the on-board readings estimate the State-of-Health 1.3% lower.

Furthermore, a sensitivity to the amount of km driven per year has been presented to strengthen the argument that for EVs, the main driver for degradation is calendar, while cycle plays a minor role. This conclusion should help to build confidence in the possibility of extending the usage of the EV not just for driving purposes but also for V2G applications, like the ones described in [15] and [16]. Moreover, the presented calendar degradation characteristics, highlighted how degradation progresses per SoC areas. This specific behaviour can be for instance used in assessing the optimal trade-off between a smart charging strategy that take advantage of local renewable energy and the corresponding additional wear caused by prolonged high SoC levels.

Finally, we wish to conclude the paper by stressing how both calendar and cycle degradation characteristics have been based on cells with similar NMC chemistry, but different size and shape. As demonstrated by the experimental results, this does not limit the validity in the approach. Future activities will extend the validation of the model over longer periods, as well as quantify the additional degradation caused by V2G services.

ACKNOWLEDGMENT

The work in this paper has been partly supported by the research project ACDC, Denmark (EUDP grant nr: 64019-0541). www.acdc-bornholm.eu

REFERENCES

- L. Calearo, M. Marinelli, C. Ziras, "A Review of Data Sources for Electric Vehicle Integration Studies," Renewable & Sustainable Energy Reviews, vol. 151, 2021.
- [2] D. Wang, J. Coignard, T. Zeng, C. Zhang, S. Saxena, "Quantifying electric vehicle battery degradation from driving vs. vehicle-to-grid services," J. Power Sources, vol. 332, 2016.
- [3] A. Zecchino, A. Thingvad, P. B. Andersen, M. Marinelli, "Suitability of Commercial V2G CHAdeMO Chargers for Grid Services," EVS 31 and EVTeC 2018.
- [4] R. Ghotge, K.P. Nijssen, J. A. Annema, J.A.; Z. Lukszo, "Use before You Choose: What Do EV Drivers Think about V2G after Experiencing It?" Energies, vol. 15, 2022.
- [5] D. Beck et al. "Inhomogeneities and Cell-to-Cell Variations in Lithium-Ion Batteries, a Review." In: Energies (2021), pages 1–25.

- [6] T. R. Tanim et al. "Fast charge implications: Pack and cell analysis and comparison." In: Journal of Power Sources 381.February (2018), pages 56–65
- [7] A. W. Thompson, Economic implications of lithium-ion battery degradation for vehicle-to- grid (V2X) services, J. Power Sources 396, 2018.
- [8] M. Marinelli, L. Calearo, J. Engelhardt, G. Rohde, "Electrical Thermal and Degradation Measurements of the LEAF e-plus 62-kWh Battery Pack," REST 22.
- [9] L. Calearo, C. Ziras, A. Thingvad, M. Marinelli, "Agnostic Battery Management System Capacity Estimation for Electric Vehicles," Energies, vol. 15, 2022.
- [10] L. Calearo, A. Thingvad, C. Ziras, M. Marinelli, "A methodology to model and validate electro-thermal-aging dynamics of electric vehicle battery packs," Journal of energy storage, vol. 55, Nov. 2022.
- [11] P. Keil et al., "Calendar Aging of Lithium-Ion Batteries,"J. Electrochem. Soc., vol. 163, no. 9, pp. A1872–A1880, 2016.
- [12] J. Wang et al., "Degradation of lithium-ion batteries employing graphite negatives and nickel-cobaltmanganese oxide+spinel manganese oxide positives: Part 1, aging mechanisms and life estimation," Journal of power sources, vol. 269, 2014.
- [13] L. Calearo, M. Marinelli, "Profitability of Frequency Regulation by Electric Vehicles in Denmark and Japan Considering Battery Degradation Costs," World Electr. Veh. J., vol. 11, 2020.
- [14] J. Engelhardt, J. M. Zepter, T. Gabderakhmanova, G. Rohde, and M. Marinelli, "Double-String Battery System with Reconfigurable Cell Topology Operated as a Fast Charging Station for Electric Vehicles," Energies, vol. 14, 2021.
- [15] P. Tsagkaroulis, A. Thingvad, M. Marinelli, K. Suzuki, "Optimal Scheduling of Electric Vehicles for Ancillary Service Provision with Real Driving Data," 2021 56th International Universities Power Engineering Conference (UPEC), 2021.
- [16] A. González-Garrido, A. Thingvad, H. Gaztañaga, M. Marinelli, "Full-Scale Electric Vehicles Penetration in the Danish Island of Bornholm – Optimal Scheduling and Battery Degradation under Driving Constraints," Journal of Energy Storage, vol. 23, pp. 381-391, June 2019.